

# A Quantum Chemical Model for Electric Field Induced Electron Transfer at Metal Electrodes. Application to Halide Oxidation on Cu(100)

David Domínguez-Ariza, Carmen Sousa, and Francesc Illas\*

*Departament de Química Física, Universitat de Barcelona and Centre Especial de Recerca en Química Teòrica / Parc Científic de Barcelona, C/Martí i Franquès 1, 08028 Barcelona, Spain*

*Received: April 15, 2002*

A model based on the use of ab initio quantum chemical explicitly correlated wave functions is proposed to study the electronic transfer reaction between an adsorbate and a metallic electrode. In this model, the effects of the electrode potential are simulated through the application of a uniform external electric field. This field exerts an influence on the relative stability of the two electronic states that are mainly involved in the electron transfer. These electronic states have the transferred electron localized either in the electrode or in the adsorbate. The model has been applied to the electron transfer between halides and a cluster model representation of the Cu(100) single-crystal electrode. A linear correlation between the electric field intensity at which the two electronic states involved in the charge-transfer process become degenerate and the normal reduction electrode potential is found. The existence of this linear correlation indicates that the proposed model contains the essential physics governing the trend of halide oxidation at a metal electrode.

## I. Introduction

Electron charge-transfer reactions either in the homogeneous phase or heterogeneous interfaces play a crucial role in many areas of chemistry<sup>1,2</sup> and biology.<sup>1,3</sup> Electron transfer reactions at electrodes are also at the heart of electrochemistry and have been intensively studied from experimental and theoretical points of view.<sup>1</sup> In the latter, the pioneering semiclassical studies by Marcus<sup>4,5</sup> and the introduction of the quantum nature of the metal surface first by Levich and Dogonadze<sup>6</sup> and later also by Marcus<sup>7</sup> represented a major breakthrough. The complexity of the electrochemical interface including the adsorbate, the solvent, and the extended metal surface makes a rigorous quantum chemical treatment almost impossible. This extraordinary complexity has triggered the appearance of simplified theoretical models that attempt to capture the essential physics of the process. Hence, many effects such as solvent, structure of the double layer, presence of specifically adsorbed ions, ionic strength, and pH are often neglected or at most treated in a very simple way. However, the resulting simplified charge transfer problem is still too difficult to reach a detailed picture by means of the methods of modern electronic structure theory. Therefore, many theoretical approaches often follow the strategy of model Hamiltonians that play an important role in various areas of solid state physics.<sup>8</sup> Here, we mention the Anderson–Newns Hamiltonian<sup>9,10</sup> for chemisorption because it has been quite extensively used to study charge-transfer reactions at electrodes.<sup>11,12</sup>

In general, all of the theoretical treatments of the charge-transfer reactions at electrodes, either assuming a given statistical mechanics model or based on the use of simplified model Hamiltonians, start from the hypothesis that any charge-transfer process can be considered as a particular case of donor–acceptor reactions. This distinctiveness comes from the fact that the electrode has the special property of having not only one orbital (or level) able to donate or to accept the transferred electron

but a continuous series of levels that define the conduction band. A general overview of most of these treatments, mainly focused on adiabatic processes, has been recently reviewed by Hush.<sup>13</sup> The common feature of all of the approaches discussed so far to describe the electronic transfer reactions on electrodes is their phenomenological character. Those are no doubt well-established theories, but precisely because of their character, the predictive capability is more limited than what is expected from a theoretical model. One of the weakest points of the phenomenological approaches is the need for a set of physically grounded parameters. In some cases, it is possible to obtain the parameters of model Hamiltonian approaches from experiment, otherwise these parameters are chosen to produce meaningful physical results. A very appealing possibility is to extract these parameters from ab initio theory applied to suitable models. This approach has been successfully applied to the description of magnetic insulators through the explicit calculation of the magnetic coupling parameter defining the Heisenberg Hamiltonian<sup>14–19</sup> and in doped high critical temperature superconducting cuprates by accurate calculation of the magnetic and electronic coupling parameters entering into the  $t$ – $J$  model Hamiltonian.<sup>20,21</sup> Precisely, the electronic coupling is one of the key properties in the theoretical models of charge-transfer processes at electrodes.<sup>6,7</sup>

In principle, the application of the ab initio techniques of quantum chemistry to charge-transfer processes at electrodes can provide reliable and unbiased parameters that can be used in forthcoming phenomenological investigations of these complicated systems. However, the application of ab initio techniques to charge-transfer processes between an adsorbate and a metallic electrode is far from being straightforward. Several theoretical, semiempirical, and ab initio studies of heterogeneous electron-transfer reactions have been reported in the specialized literature. Most of these studies use a cluster model to represent the electrode surface and a variety of computational methods, from simple extended Hückel calculations to rather sophisticated ab initio methods including Hartree–Fock and density functional

\* To whom correspondence should be addressed.

theory approaches. Zinola et al.<sup>22</sup> used the extended Hückel method to study the reduction of O<sub>2</sub> on a Pt (111) electrode. Nagy et al.<sup>23</sup> reported an interesting extended Hückel study of the electronic coupling between Au(100) and Cu/Au(100) electrodes and the red-ox Fe<sup>II</sup>/Fe<sup>III</sup> species. Nazmutdinov et al.<sup>24</sup> focused mainly on the determination of the reorganization energies and of the electronic transmission coefficient using either cluster or jellium models for the electrode. Kuznetsov et al.<sup>25–27</sup> studied the red-ox reaction of solvated H<sup>+</sup> on a Cu (100) electrode using the second-order Møller–Plesset perturbation method. In a series of papers, Anderson et al. reported Hartree–Fock calculations modeling the reduction of H<sup>+</sup> on a diamond electrode and model studies of the catalyzed reduction of O<sub>2</sub>.<sup>28–30</sup> These theoretical studies represent valuable contributions and provide the first steps toward a microscopic understanding of charge transfer at electrodes. Nevertheless, these models suffer from a series of limitations that have to be overcome before a detailed picture of this important physical process emerges. First, all of these approaches consider a single electronic state whereas charge transfer necessarily implies two (or more) electronic states simultaneously.<sup>6,7</sup> Second, the effects of the electrode potential are either neglected or represented in a rather crude way. Zinola et al.<sup>22</sup> attempt to mimic the effect of the electrode potential by monitoring the atomic parameters used in the semiempirical extended Hückel method. Anderson et al.<sup>28–30</sup> assume that the main effect of the electrode potential is to change the nuclear configuration of the donor–acceptor pair, and they artificially modify the structures to equilibrate the frontier orbitals of the red-ox pair.

In a recent paper, Hartnig and Koper<sup>31</sup> present a molecular simulation study of the solvent reorganization in electron transfer reactions and found that deviations from Marcus theory are relatively small. These authors explicitly consider the role of the solvent but in a first step ignore the role of the electric field in the electron transfer process. The present paper starts from the opposite point of view. We explicitly take into account the electric field effects on the electron transfer process but neglect the role of the solvent. This choice permits us to present an ab initio quantum chemistry based model to study the electron transfer reactions on electrodes which aims to overcome some of the limitations commented in the preceding discussion. On one hand, it permits one to take into account the multiconfigurational character of the electron transfer reaction by simultaneously treating the two electronic states. These states correspond to the two distinct physical situations in which the electron to be transferred is either in the adsorbate or on the surface. On the other hand, the present model also includes electrode potential effects by means of the application of an external uniform electric field perpendicular to the electrode surface. Many authors have explicitly included electric field effects on the properties of adsorbates.<sup>32–42</sup> The novelty of the present paper is the explicit and simultaneous consideration of the electric field effect in the two electronic states involved in the charge-transfer process. The main hypothesis of our model is that charge transfer takes place when, as a consequence of the applied external field, the two electronic states described above become degenerate. The adequacy of the model is established by comparing the electric field intensity at which the two electronic states involved in the charge-transfer process become degenerate and the equilibrium normal reduction electrode potential. We will provide evidence for the existence of a linear correlation between these two quantities. This correlation indicates that the proposed model, even neglecting the role of the solvent, contains the essential physics of the red-ox

processes at electrodes, at least for the cases considered in the present work.

## II. Proposal for an ab Initio Quantum Chemical Electron Transfer Model

In this section, we propose a model to study electric field induced electron transfer reactions at electrodes by means of ab initio quantum chemical calculations. The starting point of the present approach is the commonly used two state donor–acceptor model for intra- and intermolecular electron-transfer reactions.<sup>2</sup> In reduction reactions, the electrode acts as an electron-donor (D), whereas in oxidation processes, the electrode acts as the electron-acceptor (A). In principle, one should consider that the electrode levels that are involved in the charge-transfer process form an energy continuum near the Fermi level. However, one can assume that the main contribution to the electron-transfer comes from the energy levels close to the Fermi level. Hence, substituting the continuum of states in the Marcus theory<sup>5</sup> by a single electronic state is a reasonable approximation. This permits one to imagine the electronic transfer process at the electrode as involving two electronic states, schematically represented as DA and D<sup>+</sup>A<sup>−</sup>. Indeed, these two states correspond to the two possible resonating valence bond situations in which the electron to be transferred is either localized on D or A. In this picture, the electron transfer process takes place when the two (diabatic) electronic states become energy degenerate. This degeneracy can be caused either by a change in the nuclear configuration, as in the case of mixed valence compounds, or by an external potential, as in electrochemical systems although in the latter case the two effects are surely present.

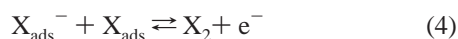
**II.A. Hypotheses of the Model.** Having established the main framework of the present model, we now describe the hypotheses that permit us to reach a fully ab initio description of the electron transfer process between an adsorbate and a metal electrode. In a first step, the role of the solvent is neglected, and we consider only electron transfer between an specifically adsorbed species and the electrode. Clearly, this is not the general case which involves species in solution; that is, the charge transfer process occurs between a species in solution with the solvation shell originally intact and the metal surface. Because the role of the solvent is not taken into account, we consider that the species involved in the electron-transfer process is adsorbed at the electrode surface and that electron transfer takes place at the equilibrium distance of the D–A ground state in absence of the external electric field. This is equivalent to assume that thermal fluctuations can be neglected in front of the electric field effects. For electrochemical systems, this implies that the present model will apply for adsorbates that have lost their solvation sphere, i.e., specifically adsorbed ions. The second hypothesis of the model is that the electron charge transfer is induced by an external potential that arises from a uniform external electric field perpendicular to the electrode surface. In general, the electric field at the double layer is not uniform, but at distances sufficiently close to the surface, the variation of the electric field is small because of the almost linear decay of the electrode potential in the solution.<sup>43,44</sup> In the framework of the two states model, the main effect of the external electric field, provided the proper electric field orientation is chosen, is to stabilize one of the considered electronic states with respect to the other until the two electronic states become degenerate. The third hypothesis assumes that the two electronic states involved in the electron transfer can be represented by ab initio multiconfigurational wave functions.

Finally, the fourth hypothesis is that a finite cluster model represents the electrode surface. This is a necessary choice because so far periodic approaches do not permit the use of multiconfigurational wave functions. From a qualitative point of view, the choice of a cluster model to represent the surface does not affect the obtained physical picture of the electron transfer process. This is because the electrode surface model does only play the role of a donor or acceptor. It is important to point out that the main hypothesis of the model discussed is also present in the well-known Marcus–Levich–Dogonadze (MLD) theory, namely, that during the electron-transfer process the Franck–Condon principle is satisfied and the electron transfer is radiationless. The main difference between the present work and previous implementations of the MLD theory is that here the condition at which the degeneracy between the pertinent electronic states is obtained from *ab initio* calculations rather than from some classical or model Hamiltonian approach.

**II.B. Application to Halide Oxidation.** It is generally assumed that the oxidation of halides at a metal anode involves two elementary steps.<sup>45</sup> In the Tafel–Volmer mechanism, these are



whereas in the Heyrovsky–Volmer mechanisms, one has



The present study focuses on the electron transfer step which is common to the two mechanisms and does not attempt to study the recombination step that completes the oxidation process. The electron transfer step assumes that the halide is already adsorbed on the anode. The present study makes use of a cluster model representation of the electrode. It is convenient to use the simplest possible model to explore the performance of different quantum chemical methods and to set up a systematic approach before using a more realistic model. The simplest possible surface model is in fact that consisting of a single metal atom which acts either as donor or acceptor. We will show that this oversimplified model leads to the same qualitative picture than a more extended surface cluster model. This conclusion will be supported from the comparison of results for the oxidation of halides induced by an external electric field obtained from two completely different anode models. These are a single  $\text{Li}^+$  cation and a  $\text{Cu}_{25}$  cluster model of the Cu(100) surface with 16 atoms in the first layer and 9 in the second one and with metal–metal distances fixed at the bulk value, cf. Figure 1. The first D–A model is then a simple  $\text{LiX}$  ( $\text{X} = \text{F}, \text{Cl}, \text{Br}, \text{and I}$ ) diatomic molecule. At the equilibrium distance, these molecules exhibit a marked ionic  $\text{Li}^+\text{X}^-$  character with the neutral electronic state lying well above in energy. The application of a uniform electric field of the right intensity in the direction of the molecular axis, hereafter referred to as  $z$ , can make the energies of the two states equal and the halide may be oxidized.<sup>46</sup> In each case, the sign of the field is chosen to model an anodic process. Obviously, this is an academic example; however, this oversimplified model provides an internal check to the hypotheses of the present charge transfer study; it permits us to establish the adequacy of the different electronic wave functions. In the more realistic  $\text{Cu}_{25}$  anode model, the halide is placed above the 4-fold hollow site. At the

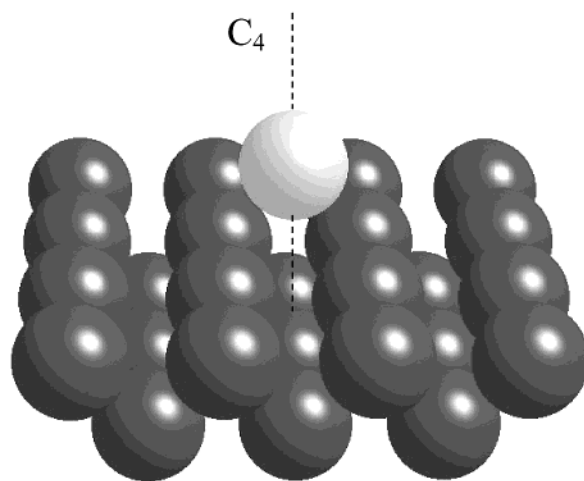


**Figure 1.** Schematic representation of the  $\text{Cu}_{25}(16,9)$  cluster model used to simulate the Cu(100) surface, a  $\text{X}^-$  halide has been added above the hollow site. The dashed line indicates the  $\text{C}_4$  symmetry axis.

equilibrium distance, the electronic ground state is dominated by the  $\text{Cu}_{25}\text{X}^-$  valence bond resonating form with the corresponding  $\text{Cu}_{25}^- \text{X}$  state well above in energy. Again, the application of an external electric field of the proper intensity in the direction perpendicular to the surface (also denoted by  $z$ ) makes the energy of the two electronic states equal and  $\text{X}^-$  can be oxidized to  $\text{X}$ .

Before starting to discuss the numerical results obtained by these two anode models, it is important to stress the similarities and differences between them. The diatomic and cluster models compare exactly; both involve halide oxidation, but in the diatomic model, the electron acceptor is  $\text{Li}^+$ , whereas in the second case, the acceptor is the neutral  $\text{Cu}_{25}$  surface cluster model. Hence, the two models mimic an electron transfer between a donor and an acceptor, and the only difference is that in one case,  $\text{Li}^+$ , the electron acceptor is a charged species. In the case of the  $\text{Li}^+$ , the electron transfer occurs between localized atomic orbitals, the  $\text{Li}(2s)$  and the  $\text{X}(\text{np}_z)$ , whereas in the case of  $\text{Cu}_{25}$ , the electron-transfer involves the  $\text{X}(\text{np}_z)$  and the highly delocalized cluster singly occupied molecular orbital, SOMO, which is essentially a combination of the  $\text{Cu}(4s)$  atomic orbitals of all cluster atoms.

**II.C. Choice of the Electronic Wave Functions.** The model for charge-transfer introduced above makes use of the DA and  $\text{D}^+\text{A}^-$  electronic states defined previously which are most often of the same space symmetry and spin multiplicity and have to be treated at the same level of accuracy. Therefore, the configuration interaction, CI, expansion of the electronic wave function becomes the appropriate choice. However, the exact full configuration interaction wave function is usually unattainable although approximate configuration interaction wave functions can still be used to obtain accurate results. The physical starting point consists of constructing a CI wave function including the DA and  $\text{D}^+\text{A}^-$  structures only. However, adding the  $\text{D}^-\text{A}^+$  structure results in a complete active space, CAS, with important computational advantages and with very small changes in the final electronic wave function for the states dominated by the DA and  $\text{D}^+\text{A}^-$  structures. The choice of a CAS simplifies the CI treatment but still leaves the problem of the orbital space. A convenient choice is to use orbitals that allow for a simultaneous and equally good description of the two electronic states. This is the state average, SA, variant of the well-known complete active space self-consistent field, CASSCF, method.<sup>47,48</sup> Here, it is important to note that the active orbitals are precisely those involved in the charge-transfer



process, and because the CASSCF and SA-CASSCF wave functions are invariant with respect to unitary transformations,<sup>49</sup> the final results are exactly the same that will be obtained by allowing for a localization of the active orbitals in the D and A fragments.

The preceding discussion about the configuration interaction approach used in this work is sufficient to understand the whole set of results presented in the forthcoming sections. However, when the electrode is simulated by a cluster model, there are several important points of technical character that may be of interest for the specialized reader. Without pretending to be exhaustive we mention the following: (i) The first electronic state is always the ground state, but the second electronic state of interest involves the computation of a highly excited root. The procedure followed to solve this problem consists simply in artificially placing the active orbitals in separate symmetry irreducible representations. (ii) The orbitals are obtained for a SA-CASSCF calculation in the absence of any external electric field, and the field effects in the CI wave functions are accounted for in the one electron integrals thus avoiding possible artifacts arising from an excessive polarization of the cluster model orbitals induced by the uniform external electric field. (iii) Dynamical electron correlation effects are not taken into account in the CASSCF or SA-CASSCF wave functions. The use of the oversimplified LiX model permits us to check the influence of the effects that are not included in the more realistic cluster models for the adsorbate–surface system.

### III. Computational Framework

The study of the diatomic models has been carried out following two different computational strategies. In the first approach, the two electronic states of interest are studied at the CASSCF and complete active space second-order perturbation theory, CASPT2,<sup>50–52</sup> levels of theory without and with the presence of the uniform external electric field. The electric field intensities that are considered are on the [0.00, –0.12] interval in atomic units. Notice that an electric field of 0.01 au corresponds to  $5.2 \times 10^7$  V cm<sup>–1</sup>, this is of the order of the electric fields encountered in electrochemical cells; an external potential of 1 V generates a field of  $\sim 10^7$  V cm<sup>–1</sup>.<sup>53</sup> In the diatomic models, the direction of the electric field follows the internuclear axis and positive fields stabilize the ionic form.

In the present calculations all electron generally contracted atomic natural orbital, ANO, basis sets have been used for Li, F, Cl, and Br,<sup>54</sup> whereas for I, the core electrons have been replaced by an *ab initio* model potential<sup>55</sup> and the 17 most external electrons have been explicitly treated in the calculations (cf. ref 56). The CAS contains two electrons and two active orbitals. The active orbitals are the molecule HOMO and LUMO which are dominantly of halogen *np<sub>z</sub>* and Li(2s) character, respectively. From the quantum chemical point of view, this is quite a limited CASSCF wave function, but it has the advantage of providing an *ab initio* version of the commonly invoked two state model for electron transfer processes. The SA-CASSCF procedure is used to obtain the molecular orbitals, and the effects of external electron correlation are included by means of the recently developed multistate CASPT2, MS–CASPT2, method<sup>57</sup> which is especially well-suited to describe near-degenerate situations such as those occurring in avoided crossings. Clearly, this first strategy is the natural choice for a molecular system. However, one must realize that the presence of an external electric field, which uniformly affects the cluster as a whole, induces a too large polarization of the outermost occupied cluster molecular orbitals involving linear combinations of the Cu(4s)

orbitals. This excessive polarization is not a consequence of using a cluster model but rather of using a uniform electric field; a periodic slab model will exhibit the same problem. Consequently, one cannot follow the route described above when the electrode is simulated by a cluster model. An alternative strategy consists of starting also from a SA-CASSCF calculation for the system in the absence of the external electric field and use these orbitals in the subsequent CASCI calculations carried out for the different electric field intensities. In this case, the influence of the electric field in the orbitals is checked by repeating the calculations but using a CI wave function that adds all single excitations to the CASCI wave function; this is denoted as CASCI+M. The comparison of results obtained following one or another computational scheme will permit us to show that both approaches are equally adequate to represent the systems of interest. The second strategy is less straightforward but can be used in the cluster model calculations.

Chemisorption and subsequent oxidation of halides on Cu-(100) has been modeled by a two-layer Cu<sub>25</sub> cluster having 16 atoms in the first layer and 9 in the second one. The halide anion is added above the cluster innermost 4-fold hollow site. The Cu<sub>25</sub> cluster model for the electrode is divided in local and outer regions as in previous works.<sup>58</sup> The five central atoms of the cluster around the hollow position define the local region and have been described with the small core effective core potential, ECP, reported by Hay and Wadt<sup>59</sup> and the corresponding double- $\zeta$  (LANL2DZ) basis set. The Cu atoms at the cluster edge have been described as one-electron pseudoatoms<sup>60</sup> and only the most external 4s electron of each Cu atom has been explicitly described with a (4s1p/2s1p) basis set. For the halogen, the primitive basis set described above has been also used but now contracted to a double- $\zeta$  plus polarization quality. The isolated Cu<sub>25</sub> cluster model has an open-shell electronic structure, whereas the halide is closed-shell. Hence, the orbitals involved are clearly the cluster SOMO and the halide *np<sub>z</sub>*. Therefore, the active space contains two orbitals as in the diatomic models. However, there are significant differences between the two active spaces. First, the CAS contains now three active electrons, and second, the halide *np<sub>z</sub>* orbital is located well below many of the cluster orbitals arising from combinations of the Cu(4s) valence orbitals. In all cases, the electric field is applied in the perpendicular direction to the surface and is considered positive when the Cu<sub>25</sub>X<sup>–</sup> form is stabilized.

The two electronic states involved in the charge transfer process have the same space symmetry and spin multiplicity and the corresponding Hamiltonian eigenfunctions experience an avoided crossing. At the crossing point, the character of each electronic state changes suddenly from DA to D<sup>+</sup>A<sup>–</sup> or vice versa. The precise determination on the avoided crossing point can be obtained by a proper diabaticization procedure. In the present work, we use the diabaticization procedure proposed by Werner and Meyer.<sup>61</sup> In this method, the character of each electronic state is determined in such a way that diabatic states are eigenfunctions of the dipole moment operator. This permits us to determine the electric field at which the avoided crossing between the two adiabatic electronic states occurs in a straightforward way.

The SA-CASSCF, CASCI, and MS–CASPT2 calculations have been performed with the MOLCAS-5 software package,<sup>62</sup> whereas CASCI+M calculations have been performed with the CASDI code.<sup>63</sup>

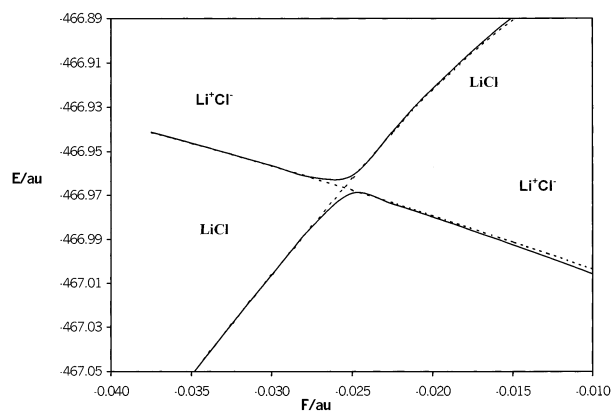


**Figure 2.** Variation of the energies of the electronic states involved in the electron transfer with the electric field intensity for LiCl at the SA-CASSCF level. Adiabatic potential energy curves are represented by solid lines whereas dashed lines correspond to the diabatic potential energy curves.

#### IV. Chemical Character of the Electronic States as a Function of the External Electric Field

In this section, we discuss the adiabatic and diabatic potential energy curves for the LiX and  $\text{Cu}_{25}\text{X}^-$  ( $\text{X} = \text{F}, \text{Cl}, \text{Br}$ , and  $\text{I}$ ) electrode-adsorbate models as a function of the intensity of the uniform external electric field, in the conditions outlined in section II. First, we will describe the simplistic diatomic model, and afterward, we will concentrate on the more realistic surface cluster model. Nevertheless, we will show that the charge transfer mechanism that shows up from the two models is essentially the same.

The variation of the energy of the DA and  $\text{D}^+\text{A}^-$  adiabatic electronic states with the external electric field intensity for LiCl at the SA-CASSCF level is shown in Figure 2 (continuous lines). Following the hypothesis of the model described in section II, the variation of the energy with respect to the electric field is carried out at the internuclear equilibrium distance which is consistent with the method and basis set chosen. Figure 2 shows that upon increasing the electric field intensity from  $-0.01$  to  $-0.04$  au the energy of the dominantly ionic  $\text{Li}^+\text{Cl}^-$  increases monotonically, whereas that of the dominantly neutral LiCl decreases, also monotonically. Notice that the fact that the negative field destabilized the ionic state is related to its orientation with respect to the molecule; a positive field will produce the same effect if the molecule is rotated by  $180^\circ$ . The dependence of the energy of the neutral and ionic electronic states with respect to the electric field can be easily rationalized from the different interaction of the molecule with the electric field in each electronic state. For the *ionic*  $\text{Li}^+\text{Cl}^-$  electronic state, the interaction with the electric field is essentially due to the net electric charges on the atoms. For the *neutral* LiCl electronic state, this interaction arises from the polarizability of the molecule and always lowers the energy; the rather large effect on the neutral state comes from the large polarizability of the halogen atom in LiCl. Therefore, with the electric field oriented as indicated above, its effect on the energy of the neutral and ionic states has the opposite direction, and hence, there must be a value of the electric field intensity,  $F_0$ , at which the energy of the two states becomes equal, cf. Figure 2. For electric fields with intensities higher than  $F_0$  (in absolute value), the two adiabatic potential energy curves exchange their behavior: the *neutral* LiCl becoming the electronic ground state. This fact is clearly evidenced by the diabatic potential energy curves, dashed lines in Figure 2, and by the dipole moment curves represented in Figure 3. The expectation values of the dipole moment

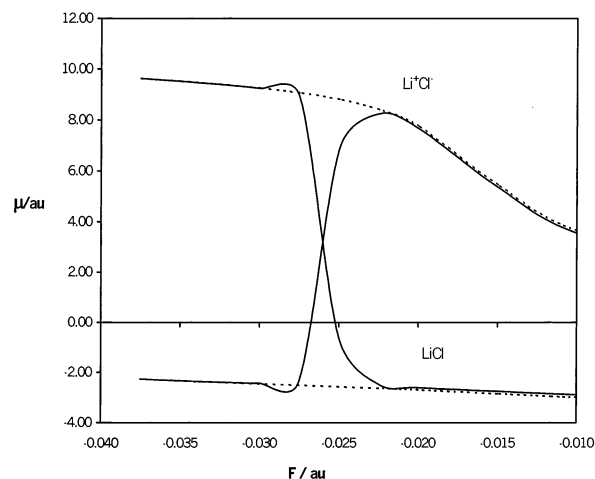


**Figure 3.** Variation of the expectation value of the dipole moment with the electric field intensity for the two electronic states of LiCl involved in the electron transfer. Solid lines stand for the expectation value of the dipole moment operator in the adiabatic basis (SA-CASSCF), whereas dashed lines correspond to the diabatic representation.

**TABLE 1: Equilibrium Distance ( $R_{\text{eq}}$ ), Vibrational Frequencies ( $\nu_{\text{eq}}$ ), and Mulliken Charges ( $Q$ ) for  $\text{X}^-$  on Cu(100) Obtained Using a  $\text{Cu}_{25}(16,9)$  Cluster Model and the Hartree–Fock Method<sup>a</sup>**

|                             | $R_{\text{eq}}/\text{\AA}$ | $\nu_{\text{eq}}/\text{cm}^{-1}$ | $Q/\text{au}$       |
|-----------------------------|----------------------------|----------------------------------|---------------------|
| $\text{Cu}_{25}\text{F}^-$  | 1.323 (1.3)                | 249 (281)                        | $-0.79$ ( $-0.55$ ) |
| $\text{Cu}_{25}\text{Cl}^-$ | 1.987 (2.0)                | 153 (178)                        | $-0.64$ ( $-0.37$ ) |
| $\text{Cu}_{25}\text{Br}^-$ | 2.202 (2.3)                | 93 (104)                         | $-0.54$ ( $-0.36$ ) |
| $\text{Cu}_{25}\text{I}^-$  | 2.484 (2.6)                | 62 (72)                          | $-0.41$ ( $-0.35$ ) |

<sup>a</sup> B3LYP results reported by Ignaczak and Gomes<sup>64</sup> using a  $\text{Cu}_{12}$  cluster model are given in parentheses.

operator plotted in Figure 3 have been obtained using either the SA-CASSCF wave function—adiabatic representation—or using the eigenfunctions of the matrix representation of the dipole moment operator in the basis of the adiabatic electronic states—diabatic representation. This diabaticization procedure permits us to obtain electronic states whose chemical character (*ionic* or *neutral*) is nearly independent of the applied field. This justifies the labels in each side of Figure 2 and the value for the  $F_0$  electric field intensity. Notice that the adiabatic dipole moment curves in Figure 3 change sharply when  $F = F_0$ , because of the change of the chemical character of the corresponding electronic states. However, in the diabatic representation, which corresponds to the dipole moment eigenstates, the dipole moment curves change smoothly with the electric field. Similar curves to those reported in Figures 2 and 3 have been obtained for the LiF, LiCl, LiBr, and LiI series at the SA-CASSCF, MS-CASPT2, CASCI, and CASCI+M levels of theory. In each case, the  $F_0$  value has been obtained as explained above. The physical significance of these values will be discussed in the next section.

The study of the halide oxidation on Cu(100) requires some preliminary calculations to determine the structural properties of adsorbed halides in the absence of the external electric field. Consequently, the adsorption of halides on Cu(100) at the hollow position has been studied at the open-shell restricted Hartree–Fock, OSRHF, level. The equilibrium distance from the halide to the surface, the vibrational frequency for the normal mode perpendicular to the surface, and the Mulliken charges on the halogen are reported in Table 1. The present OSRHF results are in good agreement with the B3LYP values reported by Ignaczak and Gomes<sup>64</sup> obtained using a  $\text{Cu}_{12}$  cluster model.

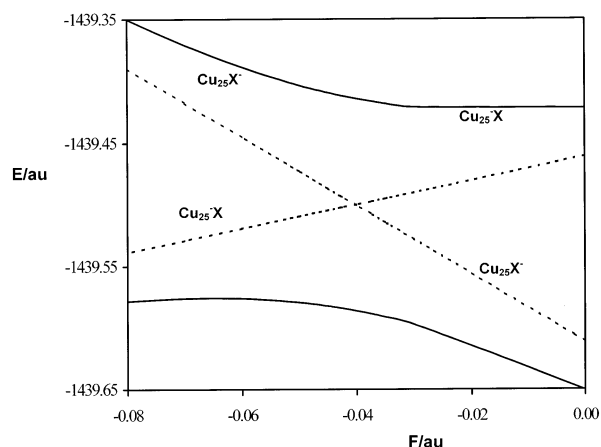


**Figure 4.** Variation of the energies of the electronic states involved in the electron transfer with the electric field intensity for  $\text{Cu}_{25}\text{Cl}^-$  at the CASCI level. Adiabatic potential energy curves are represented by solid lines whereas dashed lines correspond to the diabatic potential energy curves.

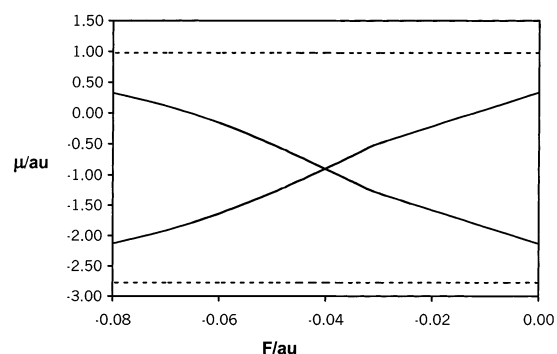


**Figure 5.** Variation of the expectation value of the dipole moment with the electric field intensity for the two electronic states of  $\text{Cu}_{25}\text{Cl}^-$  involved in the electron transfer. Solid lines stand for the expectation value of the dipole moment operator in the adiabatic basis (CASCI), whereas dashed lines correspond to the diabatic representation.

Once the structural parameters are obtained, one can proceed with the study of the electron-transfer process by placing the halide at the equilibrium distance and applying the external electric field. The study of the electronic transfer reaction has been carried out at the CASCI level and using the molecular orbitals obtained by a SA-CASSCF calculation without electric field. Figure 4 reports the evolution of the energy of the DA and  $\text{D}^+\text{A}^-$  electronic states with the electric field for the  $\text{Cu}_{25}\text{Cl}^-$  system both in the diabatic and adiabatic representation. Here, the direction of the external electric field is such that for a negative field, the negative charge is pulled toward the metal surface. Hence, increasing the electric field intensity from 0.00 to  $-0.12$  au switches the relative stability of the two electronic states of interest. Again, for an  $F_0$  electric field the energy of the two electronic states becomes equal and charge transfer can occur without further energy. The dipole moment curves reported in Figure 5 confirm the above considerations; the dipole moment curves obtained from the adiabatic states change sharply their behavior around  $F_0$ , showing the change of relative stability of the  $\text{Cu}_{25}\text{X}^-$  and  $\text{Cu}_{25}^-\text{X}$  forms. From Figure 4, the electronic coupling term needed in some model Hamiltonian approaches can be readily obtained. The computed coupling is rather large, and one may wonder whether the resulting process can be described as an electron transfer. This is because the electron transfer term is usually employed in the limit of small couplings. However, one must recall that on one hand we are dealing with a rather crude model of the real electrochemical system and,

on the other hand, the adsorbed state is considered. Further away from the surface, the coupling will be smaller, and the presence of the solvent will surely go in the same direction.

## V. Validation of the Model

From the discussion above, it appears that the present ab initio model properly predicts a charge transfer process between an electrode and a specifically adsorbed anion induced by an external electric field. Therefore, the proposed model seems to be at least qualitatively correct. However, a proper theoretical model must also be able to produce accurate predictions on a quantitative level. The key property of the present model is  $F_0$ , the electric field intensity at which charge transfer is predicted to occur. Unfortunately, the comparison between the present theoretical values for  $F_0$  and experiment is not simple and is far from being straightforward. In fact, the experimental quantity that controls red-ox processes at electrodes is the external potential although this is measured in physical conditions far from those represented in the theoretical calculations. Electrode potentials are usually measured at room temperature, on solution, and most often under thermodynamic equilibrium conditions. Moreover, the result of such a measurement is necessarily an statistical average. Nevertheless, one can attempt to relate the red-ox potentials to the calculated  $F_0$  values. To this end, it is necessary to connect the electric field with the potential. In principle one can assume that the electric field in the double-layer region is almost constant. Hence, the electrode potential,  $E$ , should vary with the electric field in a nearly linear way; i.e.,  $E = dF$  where  $d$  is the double layer thickness which to a first approximation can be taken as  $3 \text{ \AA}$ .<sup>65</sup> This hypothesis has been indirectly proven by comparison of the variation of the calculated vibrational frequency of adsorbed CO with respect to an external electric field and the experimental value for the variation of the same quantity but with respect to the electrode potential.<sup>41,66</sup> The above commented relationship between electric field at the electrode and the corresponding potential strongly suggests that  $F_0$  should be proportional to the equilibrium red-ox potential and, in particular, to the standard red-ox potential.

For the LiX model,  $F_0$  has been obtained for F, Cl, Br, and I using the different ab initio methods described above. These electric fields have been plotted versus the normal reduction electrode potential  $E_{\text{X}_2/\text{X}^-}^0$  taken from available literature data,<sup>67</sup> cf. Figure 6. The use of the  $E_{\text{X}_2/\text{X}^-}^0$  potential is justified from the halide oxidation mechanisms described in eqs 1–4 assuming that the recombination step is not influenced by the electric field. For all of the theoretical methods, a linear correlation between  $F_0$  and  $E_{\text{X}_2/\text{X}^-}^0$  is obtained and the main difference between the different results lies in the intensity of the  $F_0$  fields. The SA-CASSCF and MS-CASPT2 curves are almost parallel and have nearly the same slope. However, the slope corresponding to the CASCI method is considerably larger. The origin of this difference is mainly due to the lack of polarization effects because the molecular orbitals used to construct the CASCI wave function are not optimized for the different fields. This results in larger values of  $F_0$  compared to those predicted by the more accurate SA-CASSCF and MS-CASPT2 methods. Notice that the effect is larger for fluorine than that for iodine in agreement with the electronegativity scale. However, the effect of the electric field in the orbitals can also be taken into account by adding all single excitations to the CASCI wave function, CASCI+M. Indeed, the CASCI+M results are very close to those obtained using either the SA-CASSCF or MS-CASPT2 level indicating that the qualitative description is not



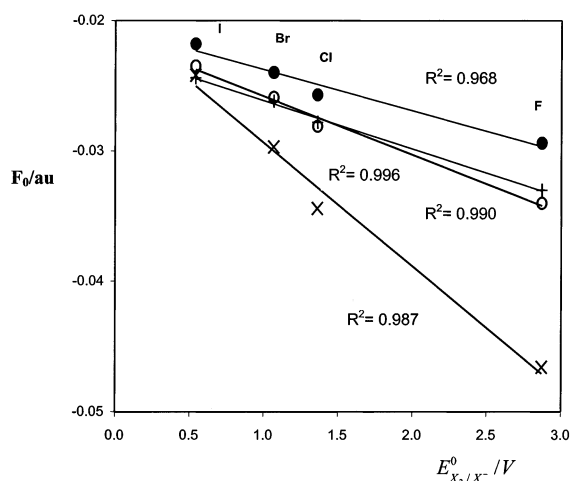


**Figure 6.** Relation between the  $F_0$  electric field (see text) and the standard equilibrium electrode potential,  $E_{X_2/X^-}^0$ , obtained at different levels of theory—SA-CASSCF (●), MS-CASPT2 (○), CASCI (×), and CASCI+M (+)—for the  $LiX$  ( $X = F, Cl, Br,$  and  $I$ ) donor–acceptor model. The square of the linear regression coefficient,  $R^2$ , is also reported.

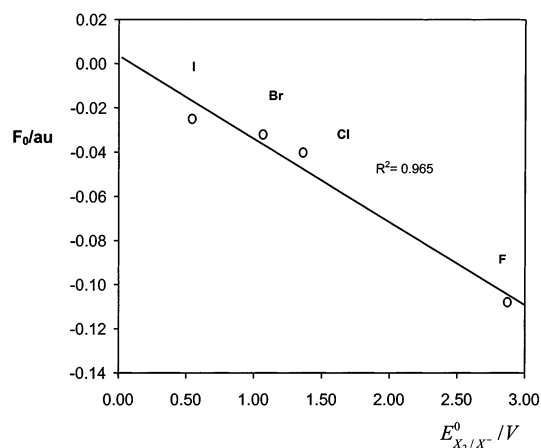


**Figure 7.** Relation between the  $F_0$  electric field (see text) and the standard equilibrium electrode potential,  $E_{X_2/X^-}^0$ , obtained at the CASCI level of theory for the  $Cu_{25}X^-$  ( $X = F, Cl, Br,$  and  $I$ ) donor–acceptor model. The square of the linear regression coefficient,  $R^2$ , is also reported.

affected by the choice of the orbitals used in the CASCI wave function. From these results, two main conclusions already emerge. First, the present proposed charge-transfer model seems to be able to provide a detailed and quantitative quantum mechanical explanation of electron-transfer reactions at electrodes. Second, all of the ab initio multiconfigurational methods employed in this work are able to describe the main features of these electron-transfer reactions. Still, one can argue that the present results are fortuitous because of the use of a too crude representation of the electrode. Results in Figure 7 for the representation of the  $F_0$  value obtained from the  $Cu_{25}X^-$  ( $X = F, Cl, Br,$  and  $I$ ) model at the CASCI level clearly show that this is not the case. Again, a linear correlation between  $F_0$  and the experimental  $E_{X_2/X^-}^0$  values is obtained. Alternatively, from  $E = dF$  one gets  $E_0 = dF_0$  for  $F = F_0$  which plotted versus  $E_{X_2/X^-}^0$  leads also to a linear correlation but with a more convenient dimensionless slope. Interestingly enough, a similar relationship between the adsorption energy of atomic oxygen on metal surfaces and the intensity of an external electric field has been previously reported.<sup>37</sup> This coincidence is due to the largely ionic character of the interaction between atomic oxygen

and metal surfaces.<sup>68</sup> Hence, both processes, atomic oxygen chemisorption and electron transfer between halides and a metal surface, are driven by electrostatics.

The existence of this linear correlation provides an indication that the proposed ab initio model for electron-transfer reactions is able to capture the main features of the physics of the electron-transfer processes on electrodes. The tendency that the larger the standard potential the larger the electric field needed to make the energy of the two states equal agrees with chemical intuition and supports the two-state model. However, there is no a priori reason to obtain a linear dependence. In fact, the analysis by Koper and Voth suggests that the mathematical dependence could be more complicated.<sup>69</sup> The fact that the dependence is linear indicates that there are no extra differential effects between the charge transfer process in one halogen or another thus validating the present quantum chemical model. For the cases considered in the present work, the role of the solvent seems not to be decisive. Nevertheless, one should consider both electric field and solvent effects. This research is currently being developed in our laboratory.<sup>70</sup>

## VI. Conclusions

A detailed ab initio quantum mechanical understanding of electric field induced electron transfer reactions between a specifically adsorbed anion and an electrode can be attained from the two state model. This requires the explicit consideration of the presence of an external electric field and the use of ab initio multiconfigurational wave functions to describe the two,  $DA$  and  $D^+A^-$ , electronic states involved in the electron-transfer process. The validity of the model has been established from the linear relationship between the electric field intensity at which the  $DA$  and  $D^+A^-$  electronic states become degenerate and the equilibrium standard red–ox potentials. The existence of this linear relationship suggests that, for these particular cases where the electron-transfer process takes place in the inner region of the double layer, the presence of the solvent has not a differential role along the halide series.

Surprisingly, the main features of the electron transfer process are not strongly influenced by the model chosen to represent the metal electrode surface, these are already apparent when the simplest electrode model is employed. The use of a more realistic cluster model representation of the electrode does only introduce minor changes in the qualitative description. Nevertheless, the use of cluster models permits us to take into account the delocalized character of the metal conduction band and will make possible to study the influence of the crystal face orientation on the red–ox processes carried out on single crystal electrodes. Other possible applications and extensions of the model involve the study of electron transfer of solvated species and the consideration of nonuniform electric fields; both are currently being investigated in our laboratory.

**Acknowledgment.** Financial support has been provided by Spanish CICyT Project PB98-1216-CO2-01 and, in part, by “Generalitat de Catalunya” Grant 2001SGR-00043. Part of the computer time was provided by the CESCA/CEPBA super-computer centers thanks to a research grant from the University of Barcelona. D.D. is indebted to the “Generalitat de Catalunya” for a predoctoral grant.

## References and Notes

- (1) Kuznetsov, A. M.; Ulstrup, J. *Electron Transfer in Chemistry and Biology: An Introduction to the Theory*, Wiley Series in Theoretical Chemistry; Wiley: New York, 1998.
- (2) Newton, M. D. *Chem. Rev.* **1991**, *91*, 767.

- (3) Marcus, R. A.; Sutin, N. *Biochim. Biophys. Acta* **1985**, *811*, 265.
- (4) Marcus, R. A. *J. Chem. Phys.* **1956**, *24*, 966.
- (5) Marcus, R. A. *J. Chem. Phys.* **1965**, *43*, 679.
- (6) Levich, V. G. In *Physical Chemistry, An Advanced Treatise*; Eyring, H., Henderson, D., Jost, W., Eds.; Academic Press: New York, 1970; Vol. Ixb.
- (7) Marcus, R. A. *Annu. Rev. Phys. Chem.* **1964**, *15*, 155.
- (8) Ashcroft, N. W.; Mermim, N. D. *Solid State Physics*; W. B. Saunders Company: New York, 1976.
- (9) Anderson, P. W. *Phys. Rev.* **1961**, *124*, 41.
- (10) Newns, D. M. *Phys. Rev.* **1969**, *178*, 1123.
- (11) Schmickler, W. *J. Electroanal. Chem.* **1986**, *204*, 31.
- (12) Schmickler, W. *Electrochim. Acta* **1995**, *41*, 2329.
- (13) Hush, N. S. *J. Electroanal. Chem.* **1999**, *470*, 170.
- (14) Illas, F.; Casanovas, J.; García-Bach, M. A.; Caballol, R.; Castell, O. *Phys. Rev. Lett.* **1993**, *71*, 3549.
- (15) Moreira, I. de P. R.; Illas, F.; Calzado, C. J.; Sanz, J. F.; Malrieu, J.-P.; Ben Amor, N.; Maynau, D. *Phys. Rev. B* **1999**, *59*, 6593.
- (16) Moreira, I. de P. R.; Illas, F. *Phys. Rev. B* **1997**, *55*, 4129.
- (17) de Graaf, C.; Illas, F. *Phys. Rev. B* **2001**, *63*, 014404.
- (18) Muñoz, D.; Illas, F.; Moreira, I. de P. R. *Phys. Rev. Lett.* **2000**, *84*, 1579.
- (19) de Graaf, C.; Moreira, I. de P. R.; Illas, F.; Martin, R. L. *Phys. Rev. B* **1999**, *60*, 3457.
- (20) Calzado, C. J.; Sanz, J. F.; Malrieu, J. P.; Illas, F. *Chem. Phys. Lett.* **1999**, *30*, 102.
- (21) Moreira, I. de P. R.; Muñoz, D.; Illas, F.; de Graaf, C.; García-Bach, M. A. *Chem. Phys. Lett.* In press.
- (22) Zinola, C. F.; Arvia, A. J.; Estiu, G. L.; Castro, E. A. *J. Phys. Chem.* **1994**, *98*, 7566.
- (23) Nagy, Z.; Curtis, L. A.; Hung, N. C.; Zurawski, D. J.; Yonco, R. M. *J. Electroanal. Chem.* **1992**, *325*, 313.
- (24) Nazmutdinov, R. R.; Tsirlina, G. A.; Petrii, O. A.; Kharkats, Y. I.; Kuznetsov, An. M. *Electrochim. Acta* **2000**, *45*, 3521.
- (25) Kuznetsov, An. M.; Lorenz, W. *Chem. Phys.* **1994**, *183*, 73.
- (26) Kuznetsov, An. M.; Lorenz, W. *Chem. Phys.* **1994**, *185*, 333.
- (27) Kuznetsov, An. M.; Lorenz, W. *Chem. Phys.* **1997**, *214*, 243.
- (28) Anderson, A. B.; Kang, D. B.; *J. Phys. Chem. A* **1998**, *102*, 5993.
- (29) Anderson, A. B.; Albu, T. V.; *J. Am. Chem. Soc.* **1999**, *121*, 11855.
- (30) Albu, T. V.; Anderson, A. B.; *Electrochim. Acta* **2001**, *46*, 3001.
- (31) Hartnig, C.; Koper, M. T. M.; *J. Chem. Phys.* **2001**, *115*, 8540.
- (32) Bagus, P. S.; Nelin, C. J.; Hermann, K.; Philpott, M. R. *Phys. Rev. B* **1987**, *36*, 8169.
- (33) Bagus, P. S.; Nelin, C. J.; Müller, W.; Philpott, M. R.; Seki, H. *Phys. Rev. Lett.* **1987**, *58*, 559.
- (34) Bagus, P. S.; Pacchioni, G. *Surf. Sci.* **1990**, *236*, 233.
- (35) Rubio, J.; Ricart, J. M.; Casanovas, J.; Blanco, M.; Illas, F. *J. Electroanal. Chem.* **1993**, *359*, 105.
- (36) Ricart, J. M.; Clotet, A.; Illas, F.; Rubio, J. *J. Chem. Phys.* **1994**, *100*, 1988.
- (37) Pacchioni, G.; Illas, F.; Neophytides, S.; Vayenas, C. G. *J. Phys. Chem.* **1996**, *100*, 16653.
- (38) Pacchioni, G.; Lomas, J. R.; Illas, F. *J. Mol. Catal.* **1997**, *119*, 263.
- (39) Curulla, D.; Clotet, A.; Ricart, J. M.; Illas, F. *Electrochim. Acta* **1999**, *45*, 639.
- (40) García-Hernández, M.; Curulla, D.; Clotet, A.; Illas, F. *J. Chem. Phys.* **2000**, *113*, 364.
- (41) Wasileski, S. A.; Weaver, M. J.; Koper, M. T. M. *J. Electroanal. Chem.* **2001**, *500*, 344.
- (42) Wasileski, S. A.; Koper, M. T. M.; Weaver, M. J. *J. Am. Chem. Soc.* **2002**, *124*, 2796.
- (43) Miller, C. J. In *Physical Electrochemistry: Principles, methods and applications*; Rubinstein, I., Ed.; Marcel-Dekker, Inc.: New York, 1995.
- (44) Brett, C. M. A.; Oliveira-Brett, A. M. *Electrochemistry: Principles, methods and applications*; Oxford University Press: New York, 1996.
- (45) Vetter, K. J. *Electrochemical Kinetics*; Academic Press: New York, 1967.
- (46) Sousa, C.; Domínguez-Ariza, D.; de Graaf, C.; Illas, F.; *J. Chem. Phys.* **2000**, *113*, 9940.
- (47) Roos, B. O.; Taylor, P. R.; Siegbahn, P. E. M. *Chem. Phys.* **1980**, *48*, 157.
- (48) Roos, B. O. In *Ab initio methods in Quantum Chemistry II*; Lawley, K. P., Ed.; John Wiley & Sons Ltd.: New York, 1987; p 399.
- (49) Roos, B. O., in *European Summerschool in Quantum Chemistry*; Ross, B. O., Widmark, P.-O., Eds.; University of Lund Chemical Centers Printshop: Lund, Sweden, 2000; p 285.
- (50) Andersson, K.; Malmqvist, P.-Å.; Roos, B. O.; Sadlej, A. J.; Wolinski, K. *J. Phys. Chem.* **1990**, *94*, 5483.
- (51) Andersson, K.; Malmqvist, P.-Å.; Roos, B. O. *J. Chem. Phys.* **1992**, *96*, 1218.
- (52) Serrano-Andrés, L.; Merchán, M.; Nebot-Gil, I.; Roos, B. O.; Fülcher, M. *J. Chem. Phys.* **1993**, *98*, 3151.
- (53) Bockris, J. O'M.; Readdy, A. K. N. *Modern Electrochemistry, Vol. II*; Plenum: New York, 1973.
- (54) Pierloot, K.; Dumez, B.; Widmark, P.-O.; Roos, B. O. *Theor. Chim. Acta* **1995**, *90*, 87.
- (55) Barandiarán, Z.; Seijo, L. *J. Chem. Phys.* **1994**, *101*, 4049.
- (56) The basis sets used in the calculations with the diatomic LiX (X = F, Cl, Br, and I) models are as follows: Li (10s4p3d/5s4p3d); F (10s4p3d/5s4p3d); Cl (13s10p4d/6s5p4d); Br (17s15p9d/7s6p5d); and I (11s10p7d/4s5p3d).
- (57) Finley, J.; Malmqvist, P.-Å.; Roos, B. O.; Serrano-Andrés, L. *Chem. Phys. Lett.* **1998**, *288*, 299.
- (58) Curulla, D.; Clotet, A.; Ricart, J. M.; Illas, F. *J. Phys. Chem. B* **1999**, *103*, 5246.
- (59) Hay, P. J.; Wadt, W. R. *J. Chem. Phys.* **1985**, *82*, 299.
- (60) Illas, F.; Rubio, J.; Barthelat, J. C. *Chem. Phys. Lett.* **1985**, *119*, 397.
- (61) Werner, H. J.; Meyer, W. *J. Chem. Phys.* **1981**, *74*, 5802.
- (62) Andersson, K.; Barisz, M.; Bernhardsson, A.; Blomberg, M. R. A.; Cooper, D. L.; Fleig, T.; Fülcher, M. P.; de Graaf, C.; Hess, B. A.; Karlström, G.; Lindh, R.; Malmqvist, P.-Å.; Neogrády, P.; Olsen, J.; Roos, B. O.; Schmmelpfennid, B.; Schültz, M.; Sadlej, A. J.; Schütz, M.; Seijo, L.; Serrano-Andrés, L.; Siegbahn, P. E. M.; Stårling, J.; Thorsteinsson, T.; Veryazov, V.; Widmark, P.-O. *MOLCAS*, version 5.1; University of Lund, Sweden, 2000.
- (63) Maynau, D.; Ben Amor, N. *CASDI* suite of programs; Toulouse, France, 1997.
- (64) Ignaczak, A.; Gomes, J. A. N. F. *J. Electroanal. Chem.* **1997**, *420*, 71.
- (65) Weaver, M. J. *Appl. Surf. Sci.* **1993**, *67*, 147.
- (66) Koper, M. T. M.; Van Santen, R. A.; Wasileski, S. A.; Weaver, M. J. *J. Chem. Phys.* **2000**, *113*, 4392.
- (67) The equilibrium standard electrode potentials have been taken from the Internet URL <http://www.webelements.com>.
- (68) Bagus, P. S.; Illas, F. *Phys. Rev. B* **1991**, *42*, 10852.
- (69) Koper, M. T. M.; Voth, G. A. *J. Chem. Phys.* **1998**, *109*, 1991.
- (70) Domínguez-Ariza, D.; Sousa, C.; Hartnig, C.; Koper, M. T. M.; Illas, F. Work in progress.